



Effect of Layer Angle on the Mechanical Properties of Epoxy-Fiberglass Composite

Mohsen Motamedi *¹, Mohammad Elahifar ¹

¹ Department of Mechanical Engineering, Faculty of Engineering, University of Isfahan, Shahreza Campus, I.R. Iran.

Abstract:

This study investigates the influence of fiber orientation angles on the mechanical performance of 7-layer epoxy/fiberglass composites under tensile loading. Given the growing demand for advanced materials in aerospace, medical, and marine applications, optimizing composite properties—such as Young's modulus and stress concentration—is critical. Using ABAQUS for finite element simulation and Design Expert software for Design of Experiments (DoE), we analyzed stress distribution and mechanical response across 30 fiber angle configurations. The Response Surface Methodology (RSM) was employed to minimize experimental runs while evaluating three key outputs: longitudinal and transverse Young's moduli and stress concentration factor (K). ANOVA results confirmed model significance ($p < 0.05$) with high R^2 values (>0.98), ensuring robust statistical fits. Quadratic and cubic models were derived for K and Young's moduli, respectively. Optimization yielded two angle sets: (36.8°, 124°, 28.4°) for balanced E_x (23.82 GPa), E_y (20.86 GPa), and K (2.68); and (83.2°, 131.6°, 61.3°) for minimized K (2.38) with $E_y > 10$ GPa (28.13 GPa). These results demonstrate that fiber angles critically govern anisotropic behavior, with specific orientations reducing stress concentrations by up to 12% while maintaining stiffness.

Article Info

Received 07 April 2025
Accepted 04 May 2025
Available online 24 May 2025

Keywords:

Polymer composite;
Mechanical properties;
Composite fiber angle;
Stress concentration;
Response Surface Methodology.

© 2025 University of Mazandaran

*Corresponding Author: m.motamedi@shr.ui.ac.ir

Supplementary information: Supplementary information for this article is available at <https://cste.journals.umz.ac.ir/>

Please cite this paper as: Motamedi, M., & Elahifar, M. (2025). Effect of layer angle on mechanical properties of epoxy-fiberglass composite. Contributions of Science and Technology for Engineering, 2(2), 9-16. doi:10.22080/cste.2025.28948.1027.

1. Introduction

The advancement of technology and the development of industries, including aerospace, medical, and marine industries, have led to an increasing demand for materials with specific properties. Composite materials, especially polymer composites, with unique characteristics such as lightweight, high hardness and strength, resistance to fracture and corrosion, and low thermal expansion coefficient, play a crucial role among synthetic materials and are widely used in various industries [1-2]. A composite material can be defined as a combination of two or more materials with distinct physical and chemical properties, resulting in a material with different properties than its components when combined, having a common interface [3]. In other words, a composite material is a combination of two or more materials that provide better properties than the individual constituents used in it [4]. In recent years, polymer composites have become one of the most significant research areas. Their high strength-to-weight ratio compared to most alloys and conventional composites makes them highly utilized and one of the most commonly used composites [5]. Stress concentration is essential in engineering design, especially in structures with discontinuities. The stress concentration factor (SCF) is

defined as the ratio of the maximum stress at a point with a discontinuity to the nominal stress at the same point without discontinuity [6]. In other words, it represents the maximum stress at an edge divided by the nominal stress at that point [7]. Composite structures with holes have been extensively used in various industrial areas for connections or other design requirements. However, the complex mechanical behavior of composite materials remains a fundamental challenge for engineers [8]. Various factors need to be considered when designing structures and engineering machines. Two vital factors are stress concentration around holes and stress intensity [9]. Understanding the impact of geometric and material parameters on stress concentration is especially important in the design of composite structures with holes [10].

Greene presented the first evaluation of SCF for orthotropic plates with a central circular hole [11]. Duan and his colleagues [12] conducted theoretical studies and physical experiments on stress concentration in glass-fiber-reinforced polypropylene composites. According to their research, the SCF is related to the hole size and increases with an increase in the hole size. Sun and his colleagues [13] investigated the effect of strain rate on tensile properties. They observed stress concentration perpendicular to the



loading direction at the hole edge and studied it. Patel and his colleagues [14] examined the influence of various discontinuities present in a plate on stress concentration. The study showed that the SCF increases when multiple holes are located close to each other in a plate. Therefore, the distance between two holes mainly affects stress concentration. Dhand and his colleagues [15] studied composites reinforced with basalt fibers. According to their research, the mechanical properties of the composite depend on the volume fraction and positioning of the reinforcing fibers. In another study, Rahman and his colleagues [16] investigated the tensile properties of polymer composites reinforced with natural and synthetic fibers. Their research indicated that the performance of polymer composites depends on the properties of the fiber, the properties of the polymer matrix, the fiber-to-matrix ratio (fiber volume fraction), and the geometry and orientation of the fibers in the composite. Prashanth and his colleagues [17] researched fiber-reinforced composites. Studies show that the main objective of fiber-reinforced composites is to produce materials with high strength and higher elastic modulus. According to the studies by Le and his colleagues [18], the addition of fibers leads to an increase in the tensile properties and tensile strength of epoxy. Moreover, Luo and his research team [19] investigated the behavior of a perforated sheet under tensile loading. They found that mechanical properties, including strength, will change by changing the fiber angle. Kumar and his research team [20] reviewed studies on stress concentration in composite panels with holes/cuts. Studies show that stress in composites also depends on factors such as fiber orientation and fiber type. Sirmour and his colleagues [21] studied open-hole testing methods for different materials. They found that fiber orientation has a significant impact on strength. The study showed that the 90-degree fiber orientation has a lower strain failure percentage compared to the 45-degree fiber orientation. Konica and his colleagues [22] modeled the failure of the phase-field for unidirectional fiber-reinforced polymer composites. The research showed that changing the fiber direction from 0 to 90 degrees reduces the material strength.

The aerospace industry is one of the industries with the most extensive use of composites. One composite-designed aircraft component is the aircraft cap or engine cover. When an aircraft cap, as shown in Figure 1, is designed as a composite and contains holes for riveting and assembly purposes, its stress concentration needs to be examined. Initially, this paper aims to investigate the effect of changing the fiber angle of the perforated composite sheet on its mechanical properties, including stress concentration factor and Young's modulus in two sheet directions under tensile testing. Then, optimization using the Design of Experiments (DOE) method is performed for two problems. In the first optimization problem, the main objective is to find an angle with the highest Young's modulus values and is close to each other in two sheet directions (E_x, E_y) with the lowest stress concentration factor (K). Then, in the second problem, the optimum angle is obtained based on the lowest stress concentration factor in the loading direction with a minimum Young's modulus of 10 GPa.



Figure 1. Aircraft cap

2. Materials and Methods

Initially, a seven-layer sheet (Fiberglass or Epoxy) was simulated using ABAQUS software for various fiber angles based on the properties of the materials used in this composite. The results were analyzed. Then, using Design Expert software, Design of Experiments (DoE) was conducted, and optimal fiber angles were obtained for two optimization cases.

2.1. Mechanical Properties of Materials

The most common fibers used in composite materials are carbon and glass fibers, which possess essential properties such as lightweight, high hardness, strength, fracture, and corrosion resistance. Considering the lower cost of glass fibers compared to carbon fibers, glass fibers are more commonly used in composite materials [23]. The simulated composite sheet consists of four epoxy layers and three glass fibers. The mechanical properties of the mentioned materials are listed in Table 1.

Table 1. Mechanical properties of the materials used in the desired composite [24-25]

Material	Tensile strength		Poisson's ratio	Shear's modulus
	E_1 (GPa)	E_2 (GPa)	ν	G_{12} (GPa)
Glass fibers	76	5	0.2	35
Epoxy	3.5	3.5	0.3	1.308

2.2. Finite Element Method

The Finite Element Method (FEM) is the most effective method for visualizing deformation and stress changes in materials or structures. It allows for predicting the maximum force that can be applied before failure or yielding [26]. In the field of structural analysis, the Finite Element Method is recognized as the most powerful, efficient, and versatile numerical method [27]. This study simulated a standard 25×250 mm composite sheet using the Finite Element Method with ABAQUS software in three stages [28].

In the first stage, analysis was performed on a rectangular sheet with standard dimensions, where one side was fixed and the other was displaced by 5 millimeters. The desired piece was then meshed using the S4R element with a grain size of two millimeters. After conducting various tests with different fiber angles, stress and strain values were extracted. Then, based on Hooke's law (Equation 1), the tensile strength of the sheet in the longitudinal direction (E_x) was investigated.

$$\sigma_1 = E_x \varepsilon_1 \tag{1}$$

In this equation, σ_1 represents the tensile stress in the longitudinal direction of the sheet, E_x is Young's modulus in the longitudinal direction, and ε_1 is the longitudinal strain of the sheet.

In the second stage, analysis was performed on the sheet with one side fixed and the other side displaced by 0.5 millimeters. Similar to the first stage, various tests were conducted with different fiber angles, and stress and strain values were extracted. The tensile strength of the sheet in the transverse direction (E_y) was then investigated using Equation 2.

$$\sigma_2 = E_y \varepsilon_2 \tag{2}$$

In this equation, σ_2 represents the tensile stress in the transverse direction of the sheet, E_y is Young's modulus in the transverse direction, and ε_2 is the transverse strain of the sheet.

In the third stage, stress concentration factors were examined. The dimensions of the sheet were the same as in the first step, but a hole with a diameter of 5 millimeters was created at its center. Using the division of stress values around the hole by the stress value simulated in the first phase, the stress concentration factor (K) was calculated using Equation 3. Figure 2 shows the simulated sheet.

$$K = \frac{\sigma_1^*}{\sigma_1} \tag{3}$$

In this equation, K is the stress concentration factor, σ_1^* is the maximum stress in the longitudinal direction of the sheet with the hole, and σ_1 is the maximum stress in the longitudinal direction of the plain sheet.

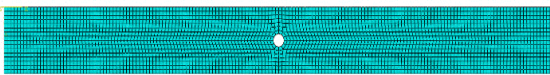


Figure 2. Simulated sheet

2.3. Design of Experiments (DoE)

Design of Experiments (DoE) is a statistical method for optimizing the performance of systems with known input variables [29]. The experiment design was carried out using Design Expert software. The effect of changing the fiber angle of the composite sheet with three input angles (in degrees) on three output parameters, namely Young's modulus in the transverse direction (in GPa), Young's modulus in the longitudinal direction (in GPa), and stress concentration factor, was investigated using the Response Surface Methodology (RSM). RSM is commonly used for designing experiments and minimizes the number of experiments needed for specific factors and their levels [30]. In this experiment, the first input parameter (angle one) was selected between 0 and 90 degrees, the second parameter (angle two) was selected between 90 and 180 degrees, and the third parameter (angle three) was selected between 0 and 90 degrees. Thirty different configurations were examined

for this experiment. The input parameters, along with their variation ranges, are presented in Table 2.

Table 2. Input parameters with a range of variations

Input parameter	Name	Type	Min	Max
A	The angle of the fibers in the first layer	Numerical	0	90
B	The angle of the fibers in the second layer	Numerical	90	180
C	The angle of the fibers in the third layer	Numerical	0	90

3. Results

3.1. Simulation Results in Abaqus

After completing the simulation stages, the selected experiments were conducted in Design Expert software, and the required parameters, including Young's modulus in both directions of the sheet and the stress concentration factor, were obtained. Table 3 shows the results obtained from the selected experiments.

Table 3. Results obtained from selected experiments

exp	Input parameter			Output parameter		
	A	B	C	K	E_x (GPa)	E_y (GPa)
1	0	90	0	2.61	24.6	14.5
2	0	112.5	22.5	2.68	26.32	15.54
3	0	135	45	2.73	25.89	14.16
4	0	157.5	67.5	2.7	20.28	9.49
5	0	180	90	2.65	17.64	7.45
6	22.5	90	0	2.63	23.8	15.79
7	22.5	112.5	22.5	2.66	26.14	17.21
8	22.5	135	45	2.71	25.87	18.94
9	22.5	157.5	67.5	2.66	20.26	15.65
10	22.5	180	90	2.63	17.57	12.02
11	45	90	0	2.57	17.56	17.23
12	45	112.5	22.5	2.62	21.63	20.3
13	45	135	45	2.67	23.95	25.38
14	45	157.5	67.5	2.61	19.63	23.49
15	45	180	90	2.55	16.78	20.42
16	67.5	90	0	2.43	10.08	17.67
17	67.5	112.5	22.5	2.50	14	21.92
18	67.5	135	45	2.57	18	28.11
19	67.5	157.5	67.5	2.5	17.12	26.28
20	67.5	180	90	2.44	15.3	24.22
21	90	90	0	2.35	7.39	17.72
22	90	112.5	22.5	2.42	9.47	22.17
23	90	135	45	2.48	13.83	28.37
24	90	157.5	67.5	2.43	15.07	26.49
25	90	180	90	2.36	14.46	24.68
26	90	90	90	2	4.31	34.85
27	0	112.5	0	2.68	26.69	14.07
28	0	135	0	2.79	31.25	11.12
29	0	157.5	0	2.9	34.41	6.35

In Experiment 30, the stress concentration factor (K) and Young's modulus in the longitudinal direction (E_x) have their highest values, while Young's modulus in the transverse direction (E_y) has its lowest value. However, in Experiment 26, the stress concentration factor and Young's modulus in the longitudinal direction have their lowest values, while Young's modulus in the transverse direction has its highest value. Based on the results of these two experiments, it can be concluded that if the fiber angle aligns with the loading direction, K and E_x have their highest values, and if the fiber angle is perpendicular to the loading direction, K and E_x have their lowest values. Berrahou et al. [31] also investigated the effect of fiber orientation in different types of composite plates with a modified U-shaped notch using composite patches. They reached the same conclusion that in polymer-based composites, fiber orientation in the direction of the applied

force results in the highest tensile strength, and the number of composite layers has a direct relationship with tensile strength.

3.2. Statistical Fit

In this experiment, variance (ANOVA) values were analyzed for the three parameters shown in Tables 4 to 6. The ANOVA table for parameter K showed a quadratic reduction, and a cubic model reduction was determined for the other two responses. The high F-values for all three responses and P-values less than 0.05 in all responses indicate the tested model's significance (sig) and the input values' accuracy. Table 7 displays the overall statistical fit of the experiment for the three responses. In this table, the R-Square values are very close to 1 and have desirable values. The closer R-Square values are to 1, the better the model fits the experimental data with less discrepancy, indicating higher precision in the experiment [32].

Table 4. Analysis of variance for stress concentration factor

Source	Sum of Square	df	Mean Square	F-value	P-value	
Model	0.9310	7	0.1330	249.62	< 0.0001	sig
A-A	0.2555	1	0.2555	479.53	< 0.0001	
B-B	0.2057	1	0.2057	386.06	< 0.0001	
C-C	0.2009	1	0.2009	377.16	< 0.0001	
AB	0.0302	1	0.0302	56.61	< 0.0001	
AC	0.0369	1	0.0369	69.28	< 0.0001	
BC	0.0400	1	0.0400	75.04	< 0.0001	
A ²	0.0151	1	0.0151	28.36	< 0.0001	
Residual	0.0117	22	0.0005			
Cor Total	0.9427	29				

Table 5. Analysis of variance for longitudinal Young's Modulus

Source	Sum of Square	df	Mean Square	F-value	P-value	
Model	1.562E+21	7	2.232E+20	140.99	< 0.0001	sig
A-A	1.031E+20	1	1.031E+20	65.16	< 0.0001	
B-B	1.668E+20	1	1.668E+20	105.38	< 0.0001	
C-C	2.004E+20	1	2.004E+20	126.62	< 0.0001	
AB	1.416E+20	1	1.416E+20	89.49	< 0.0001	
BC	1.521E+20	1	1.521E+20	96.07	< 0.0001	
A ²	2.153E+19	1	2.153E+19	13.60	0.0013	
A ³	1.158E+19	1	1.158E+19	7.32	0.0129	
Residual	3.482E+19	22	1.583E+18			
Cor Total	1.597E+21	29				

Table 6. Analysis of variance for Transverse Young's Modulus

Source	Sum of Square	df	Mean Square	F-value	P-value	
Model	1.451E+21	9	1.612E+20	85.88	< 0.0001	sig
A-A	2.564E+20	1	2.564E+20	136.61	< 0.0001	
B-B	2.709E+18	1	2.709E+18	1.44	0.2436	
C-C	2.163E+19	1	2.163E+19	11.52	0.0029	
AB	8.128E+19	1	8.128E+19	43.31	< 0.0001	
AC	1.148E+18	1	1.148E+18	0.6114	0.4434	

BC	9.955E+19	1	9.955E+19	53.04	< 0.0001
A ²	3.330E+19	1	3.330E+19	17.74	0.0004
ABC	8.280E+18	1	8.280E+18	4.41	0.0486
A ² B	1.013E+19	1	1.013E+19	5.39	0.0309
Residual	3.754E+19	20	1.877E+18		
Cor Total	1.488E+21	29			

Table 7. Statistical Fit of experiment

Response	R ²	Adjusted R ²	Predicted R ²	Adequate Precision
K	0.9876	0.9836	0.9696	80.4722
E _x	0.9782	0.9713	0.9560	48.4089
E _y	0.9748	0.9634	0.9523	38.3150

3.3. Mathematical Models

After designing experiments and analyzing the obtained results, the values for the analysis of variance tables were determined. Then, the mathematical model for stress concentration factor, Young's modulus in the longitudinal direction, and Young's modulus in the transverse direction were defined as follows. In all three models, parameter A represents the angle of the fibers in the first layer, parameter B represents the angle of the fibers in the second layer, and parameter C represents the angle of the fibers in the third layer (glass fibers).

3.3.1. Stress concentration factor, K:

$$K = 2.27788 - 0.00461778 A + 0.00383555 B + 0.00479104 C + 4.66342 \times 10^{-5} AB - 4.92444 \times 10^{-5} AC - 4.65192 \times 10^{-5} BC - 2.85977 \times 10^{-5} A^2 \quad (4)$$

3.3.2. Longitudinal Young's Modulus, E_x:

$$E_x = 1.52165 \times 10^{10} - 1.75964 \times 10^8 A + 1.12803 \times 10^8 B + 1.78403 \times 10^8 C + 2.14793 \times 10^6 AB - 2.19545 \times 10^6 BC - 5.76054 \times 10^6 A^2 + 35017.7 A^3 \quad (5)$$

3.3.3. Transverse Young's Modulus, E_y:

$$E_y = 2.63626 \times 10^{10} - 4.42564 \times 10^8 A - 1.21182 \times 10^8 B + 2.63296e \times 10^8 C + 5.42688 \times 10^6 AB + 2.53044 \times 10^6 AC - 1.38939 \times 10^6 BC + 1.75893 \times 10^6 A^2 - 20789.5 ABC - 22989.2 A^2 B \quad (6)$$

3.4. Graphical Analysis of Modeling

Figure 3-a shows the response surface plots for the stress concentration factor (K). The results indicate that when the third parameter (angle of the fibers in the third layer) is maintained at the intermediate level (45 degrees), the stress concentration factor decreases with an increase in the angle of the fibers in the first layer and a decrease in the angle of the fibers in the second layer.

Figure 3-b displays the response surface plots for Young's modulus in the longitudinal direction (E_x). The results show that when the third parameter (angle of the fibers in the third layer) is maintained at the intermediate level (45 degrees), Young's modulus in the longitudinal direction increases with a decrease in the angle of the fibers in the first layer and an increase in the angle of the fibers in the second layer.

Figure 3-c illustrates the response surface plots for Young's modulus in the transverse direction (E_y). The results indicate that when the third parameter (angle of the fibers in the third layer) is maintained at the intermediate level (45 degrees), Young's modulus in the transverse direction increases with an increase in the angle of the fibers in the first layer and a decrease in the angle of the fibers in the second layer.

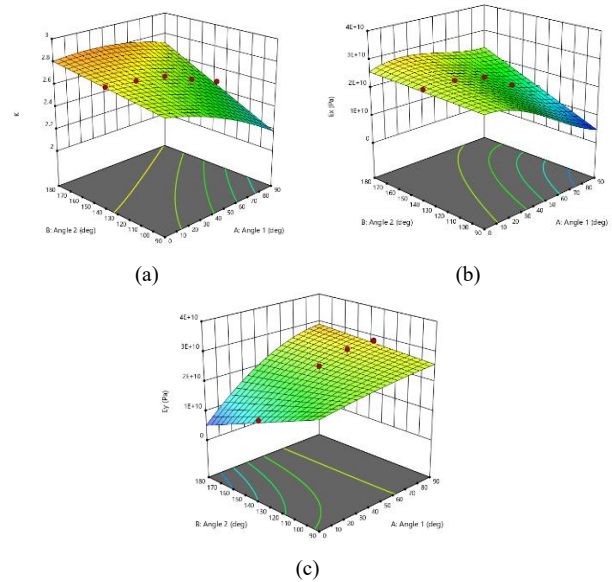


Figure 3. Response surface plots for output parameters a) stress concentration factor, b) Young's modulus in the longitudinal direction, c) Young's modulus in the transverse direction

3.5. Comparison of Predicted and Actual Values

The chart depicting the comparison between predicted and actual values in the Design Expert software indicates the level of agreement between predicted and real values. This chart is used to assess the performance of an algorithm or

prediction model. Figure 4 shows the comparison chart of predicted and actual values for all three output parameters of the experiment.

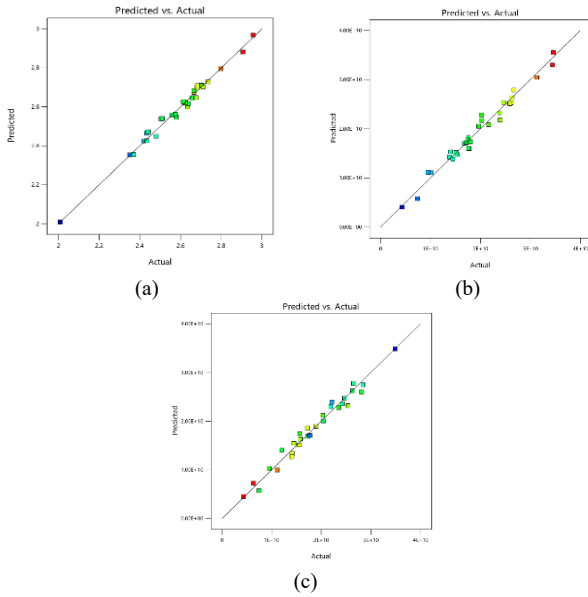


Figure 4. Comparison plots of predicted and actual values for Output parameters: a) stress concentration factor, b) Young's modulus in the longitudinal direction, c) Young's modulus in the transverse direction

3.6. Optimization

After analyzing the results, the Design Expert software provided the optimal angles for the two problem scenarios. Tables 8 and 9 show the input and output parameters, along with the optimization conditions and variation ranges for each parameter. These tables also show the final responses of the experiment and the values of the output parameters.

In the first problem, the main optimization objective is to find an angle that maximizes Young's modulus while keeping the stress concentration factor (K) minimized and close to each other in two sheet directions (E_x, E_y). In the second problem, the primary goal is to find the optimal angle based on the lowest stress concentration factor under loading, with a minimum Young's modulus of 10 GPa.

Table 8. Input and output parameters along with optimization conditions for the first problem

Name	Goal	Lower Limit	Upper Limit	Solution
A: Angle1 (deg)	is in range	0	90	36.8
B: Angle2 (deg)	is in range	90	180	124
C: Angle3 (deg)	is in range	0	90	28.4
K	minimize	2	2.95	2.68
E_x (GPa)	maximize	4.31	34.59	23.82
E_y (GPa)	maximize	4.35	34.86	20.86

Table 9. Input and output parameters along with optimization conditions for the second problem

Name	Goal	Lower Limit	Upper Limit	Solution
A: Angle1 (deg)	is in range	0	90	83.2
B: Angle2 (deg)	is in range	90	180	131.6
C: Angle3 (deg)	is in range	0	90	61.3
K	minimize	2	2.95	2.38
E_x (GPa)	maximize	4.31	34.59	12.47
E_y (GPa)	maximize	4.35	34.86	28.13

A: Angle1 (deg)	is in range	0	90	83.2
B: Angle2 (deg)	is in range	90	180	131.6
C: Angle3 (deg)	is in range	0	90	61.3
K	minimize	2	2.95	2.38
E_x (GPa)	maximize	4.31	34.59	12.47
E_y (GPa)	maximize	4.35	34.86	28.13

4. Conclusion

This paper investigated the effect of changing fiber angles on the stress concentration of a composite 7-layer perforated sheet under tensile loading using Design of Experiments (DoE). Based on the results and optimization conditions for the two problem cases, the following conclusions were obtained:

When the fibers are aligned with the loading direction, the maximum value of Young's modulus in the loading direction will be achieved.

When the fibers are perpendicular to the loading direction, the minimum stress concentration factor in the loading direction will be achieved.

For the first problem case, the optimal angles were found to be $(36.8^\circ, 124^\circ, 28.4^\circ)$ or equivalently $(36.8^\circ, -56^\circ, 28.4^\circ)$ with Young's modulus values in the two directions of the sheet and stress concentration factor of (23.82 GPa, 20.86 GPa, 2.68).

For the second problem case, the optimal angles were found to be $(83.2^\circ, 131.6^\circ, 61.3^\circ)$ or equivalently $(83.2^\circ, -48.4^\circ, 61.3^\circ)$ with Young's modulus values in the two directions of the sheet and stress concentration factor of (12.47 GPa, 28.13 GPa, 2.38).

5. References

- [1] Yang, G., Park, M., & Park, S. J. (2019). Recent progresses of fabrication and characterization of fibers-reinforced composites: A review. *Composites Communications*, 14, 34–42. doi:10.1016/j.coco.2019.05.004.
- [2] Pendhari, S. S., Kant, T., & Desai, Y. M. (2008). Application of polymer composites in civil construction: A general review. *Composite Structures*, 84(2), 114–124. doi:10.1016/j.compstruct.2007.06.007.
- [3] Hasan, M., Zhao, J., & Jiang, Z. (2019). Micromanufacturing of composite materials: A review. *International Journal of Extreme Manufacturing*, 1(1), 12004. doi:10.1088/2631-7990/ab0f74.
- [4] Khayal, O. M. E. S. (1998). Updated Curriculum Vitae. PhD Thesis, Sudan University of Science and Technology, Khartoum, Sudan.
- [5] Sinha, A. K., Narang, H. K., & Bhattacharya, S. (2020). Mechanical properties of hybrid polymer composites: a review. *Journal of the Brazilian Society of Mechanical Sciences and Engineering*, 42(8), 431. doi:10.1007/s40430-020-02517-w.

- [6] Nziu, P. K., & Masu, L. M. (2019). Cross bore geometry configuration effects on stress concentration in high-pressure vessels: a review. *International Journal of Mechanical and Materials Engineering*, 14(1), 6. doi:10.1186/s40712-019-0101-x.
- [7] Rezaeepazhand, J., & Jafari, M. (2005). Stress analysis of perforated composite plates. *Composite Structures*, 71(3–4), 463–468. doi:10.1016/j.compstruct.2005.09.017.
- [8] Özaslan, E., Yetgin, A., Acar, B., & Güler, M. A. (2021). Damage mode identification of open hole composite laminates based on acoustic emission and digital image correlation methods. *Composite Structures*, 274, 114299. doi:10.1016/j.compstruct.2021.114299.
- [9] Hsu, C. W., & Hwu, C. (2021). A special boundary element for holes/cracks in composite laminates under coupled stretching-bending deformation. *Engineering Analysis with Boundary Elements*, 133, 30–48. doi:10.1016/j.enganabound.2021.08.016.
- [10] Bayati Chaleshtari, M. H., & Khoramishad, H. (2022). Investigation of the effect of cutout shape on thermal stresses in perforated multilayer composites subjected to heat flux using an analytical method. *European Journal of Mechanics, A/Solids*, 91, 104412. doi:10.1016/j.euromechsol.2021.104412.
- [11] Rahmouni, F., Elajrami, M., Madani, K., & Campilho, R. D. S. G. (2023). Isogeometric analysis of stress concentrations and failure strength in composite plates with circular holes using RHT-splines. *European Journal of Mechanics-A/Solids*, 99, 104904. doi:10.1016/j.euromechsol.2022.104904.
- [12] Duan, S., Zhang, Z., Wei, K., Wang, F., & Han, X. (2020). Theoretical study and physical tests of circular hole-edge stress concentration in long glass fiber reinforced polypropylene composite. *Composite Structures*, 236, 111884. doi:10.1016/j.compstruct.2020.111884.
- [13] Sun, J., Jing, Z., Wu, J., Wang, W., Zhang, D., & Zhao, J. (2020). Strain rate effects on dynamic tensile properties of open-hole composite laminates. *Composites Communications*, 19, 226–232. doi:10.1016/j.coco.2020.04.004.
- [14] Patel, R. H., & Patel, B. P. (2022). Effect of various discontinuities present in a plate on stress concentration: a review. *Engineering Research Express*, 4(3), 32001. doi:10.1088/2631-8695/ac8c1b.
- [15] Dhand, V., Mittal, G., Rhee, K. Y., Park, S. J., & Hui, D. (2015). A short review on basalt fiber reinforced polymer composites. *Composites Part B: Engineering*, 73, 166–180. doi:10.1016/j.compositesb.2014.12.011.
- [16] Rahman, R., & Zhafer Firdaus Syed Putra, S. (2019). Tensile properties of natural and synthetic fiber-reinforced polymer composites. *Mechanical and Physical Testing of Biocomposites, Fibre-Reinforced Composites and Hybrid Composites*, 81–102, Woodhead Publishing, Sawston, United Kingdom. doi:10.1016/b978-0-08-102292-4.00005-9.
- [17] Prashanth, S., Subbaya, K. M., Nithin, K., & Sachhidananda, S. (2017). Fiber reinforced composites-a review. *J. Mater. Sci. Eng*, 6(03), 2-6.
- [18] Le, T. M., & Pickering, K. L. (2015). The potential of harakeke fibre as reinforcement in polymer matrix composites including modelling of long harakeke fibre composite strength. *Composites Part A: Applied Science and Manufacturing*, 76, 44–53. doi:10.1016/j.compositesa.2015.05.005.
- [19] Luo, H., Wang, H., Zhao, Z., Xue, H., & Li, Y. (2023). Experimental and numerical investigation on the failure behavior of Bouligand laminates under off-axis open-hole tensile loading. *Composite Structures*, 313, 116932. doi:10.1016/j.compstruct.2023.116932.
- [20] Kumar, S. A., Rajesh, R., & Pugazhendhi, S. (2020). A review of stress concentration studies on fibre composite panels with holes/cutouts. *Proceedings of the Institution of Mechanical Engineers, Part L: Journal of Materials: Design and Applications*, 234(11), 1461–1472. doi:10.1177/1464420720944571.
- [21] Sirmour, S., Kumar, U., Chandrakar, H., & Gupta, N. (2019). Open Hole Testing Methods for Different Materials: A Review. *IOP Conference Series: Materials Science and Engineering*, 561(1), 012037. doi:10.1088/1757-899x/561/1/012037.
- [22] Konica, S., & Sain, T. (2023). Phase-field fracture modeling for unidirectional fiber-reinforced polymer composites. *European Journal of Mechanics, A/Solids*, 100, 105035. doi:10.1016/j.euromechsol.2023.105035.
- [23] Altin Karataş, M., & Gökçaya, H. (2018). A review on machinability of carbon fiber reinforced polymer (CFRP) and glass fiber reinforced polymer (GFRP) composite materials. *Defence Technology*, 14(4), 318–326. doi:10.1016/j.dt.2018.02.001.
- [24] Van Quy, H. O., & Nguyen, S. T. T. (2019). Experimental Analysis of Coir Fiber Sheet Reinforced Epoxy Resin Composite. *IOP Conference Series: Materials Science and Engineering*, 642(1), 12007. doi:10.1088/1757-899X/642/1/012007.
- [25] Çuvalci, H., Erbay, K., & İpek, H. (2014). Investigation of the Effect of Glass Fiber Content on the Mechanical Properties of Cast Polyamide. *Arabian Journal for Science and Engineering*, 39(12), 9049–9056. doi:10.1007/s13369-014-1409-8.
- [26] Azmi, N. N., Mohd Radi, M. B. A., Muhammad Taufik, M. H. N., Adnan, N., Minhuaazam, L. N., & Mahmud, J. (2023). The effects of open hole and fiber orientation on Kevlar/Epoxy and Boron/Epoxy composite laminates under tensile loading. *Materials Today: Proceedings*, 75, 169–172. doi:10.1016/j.matpr.2022.11.220.
- [27] Marinkovic, D., & Zehn, M. (2019). Survey of finite element method-based real-time simulations. *Applied Sciences (Switzerland)*, 9(14), 2775. doi:10.3390/app9142775.
- [28] Toubal, L., Karama, M., & Lorrain, B. (2005). Stress concentration in a circular hole in composite plate.

Composite Structures, 68(1), 31–36.
doi:10.1016/j.compstruct.2004.02.016.

- [29] Uy, M., & Telford, J. K. (2009). Optimization by Design of Experiment techniques. 2009 IEEE Aerospace Conference, 1–10. doi:10.1109/aero.2009.4839625.
- [30] Chelladurai, S. J. S., K., M., Ray, A. P., Upadhyaya, M., Narasimharaj, V., & S., G. (2021). Optimization of process parameters using response surface methodology: A review. *Materials Today: Proceedings*, 37, 1301–1304. doi:10.1016/j.matpr.2020.06.466.
- [31] Mohamed, B., Khaoula, A., & Leila, B. (2023). Effect of the Fibers Orientation of the Different Types of Composite Plates Notched of U-Shape Repaired by Composite Patch. *Materials Research*, 26, 20220302. doi:10.1590/1980-5373-MR-2022-0302.
- [32] Yunardi, Y., Zulkifli, Z., & Masrianto, M. (2011). Response Surface Methodology Approach to Optimizing Process Variables for the Densification of Rice Straw as a Rural Alternative Solid Fuel. *Journal of Applied Sciences*, 11(7), 1192–1198. doi:10.3923/jas.2011.1192.1198.